Supplementary Information (SI)

A Lightweight, Li Supplementary and Lithiophilic Interface Enables high Energy Density Anode-Less Lithium Metal Batteries

Lu Cheng [a], Jiacheng Liu [a], Helin Wang [a], Yuxiang Guo [a], Ahu Shao [a], Yunsong Li [a], Zhiqiao Wang [a], Yaxin Zhang [a], Jiawen Tang [a], Chunwei Li [a], and Yue Ma [a]*

[a] State Key Laboratory of Solidification Processing, Center for Nano Energy Materials, School of Materials Science and Engineering, Shaanxi Joint Laboratory of Graphene, Northwestern Polytechnical University, Xi'an 710072, P. R. China.

Corresponding author: mayue04@nwpu.edu.cn (Y. Ma)

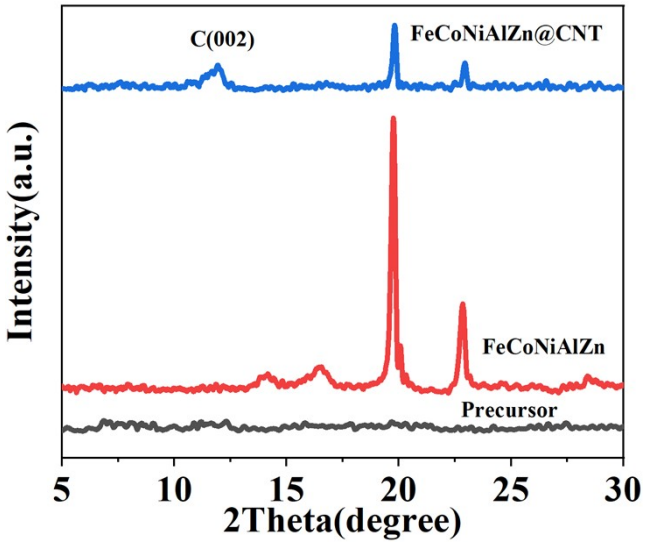

Fig. S1.XRD pattern of precursor, FeCoNiAlZn and FeCoNiAlZn@CNT.

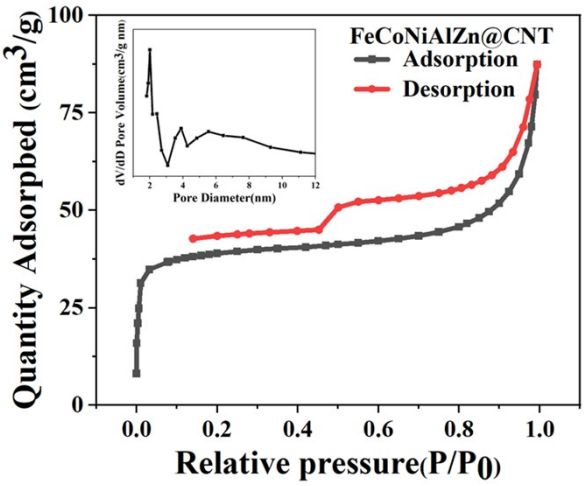

Fig. S2. N_2 adsorption–desorption isotherms and (inset) the corresponding pore size distribution of FeCoNiAlZn@CNT.

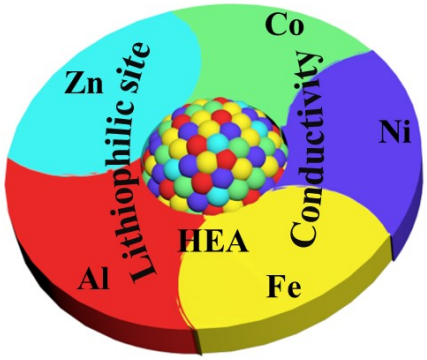

Fig. S3. Rational design of elementary selection for the HEA synthesis.

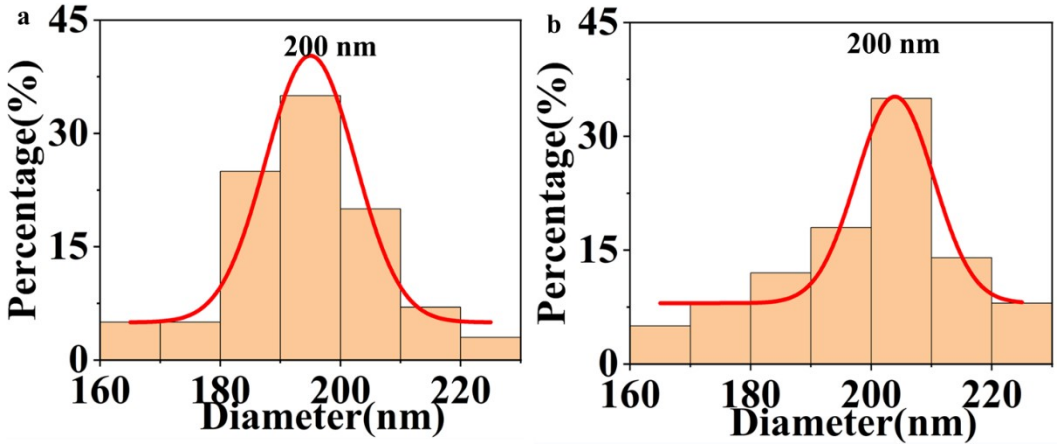

Fig. S4. The statistics of the size distribution of (a) the Sn and (b) $Li_{22}Sn_5$.

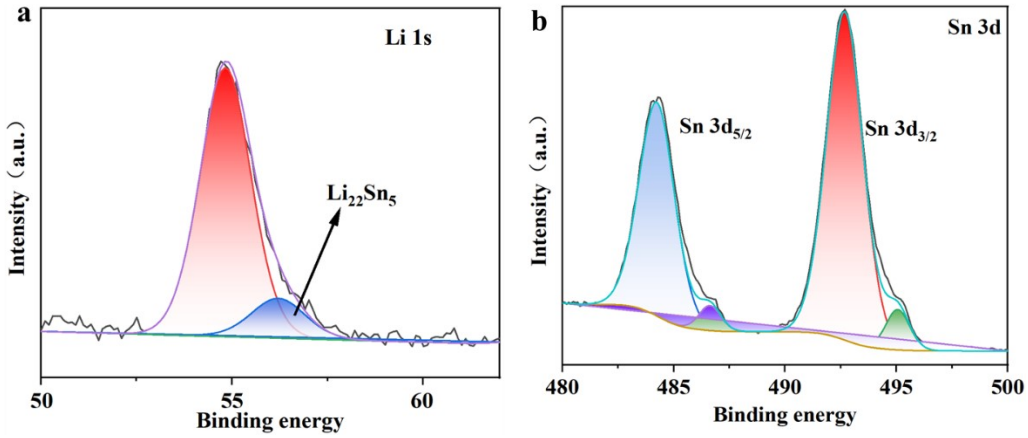

Fig. S5. High-resolution XPS spectra of (a) the Li 1s and (b) Sn 3d for the $Li_{22}Sn_5$.

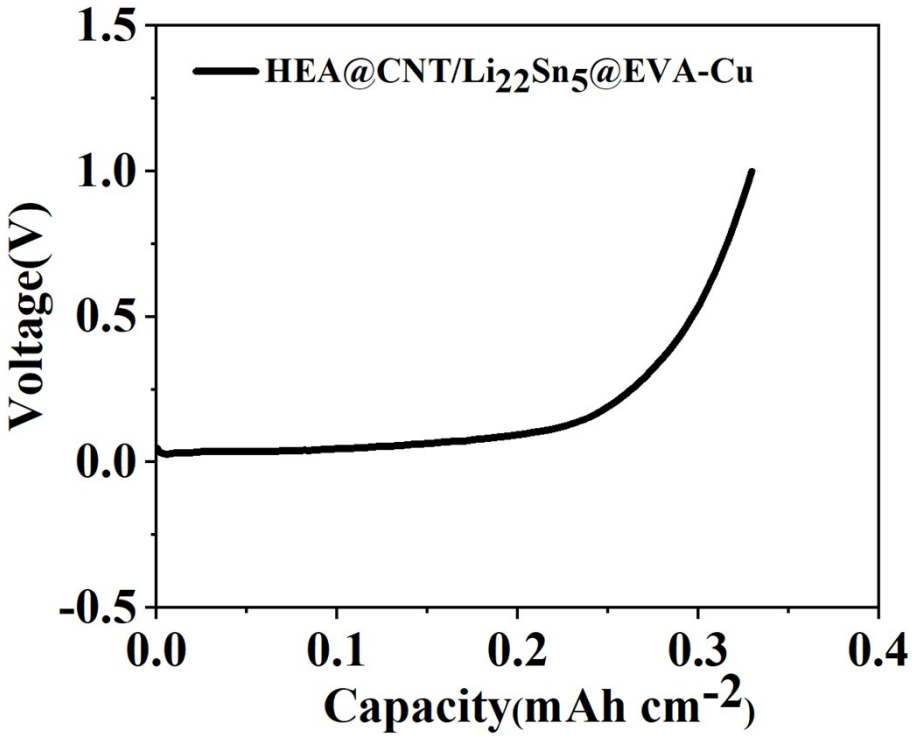

Fig. S6. Lithium inventories of HEA@CNT/$Li_{22}Sn_5$@EVA-Cu electrode after the first cycle measured by galvanostatic charging.

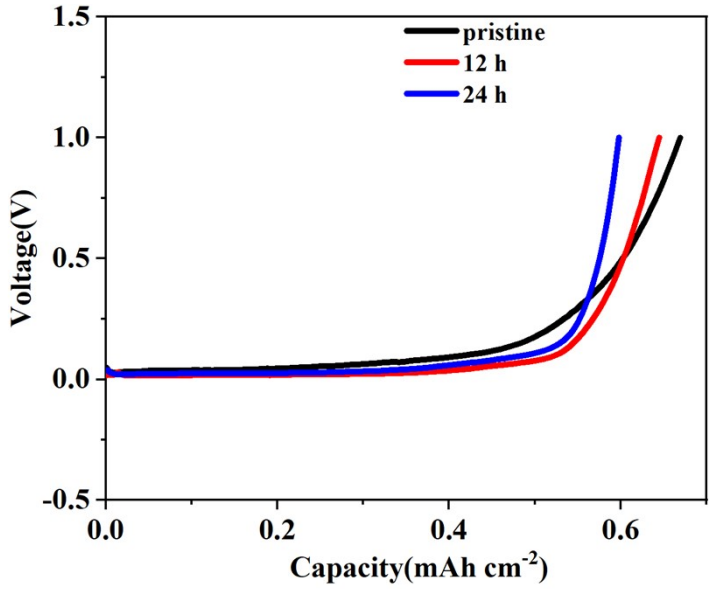

Fig. S7. The retrievable capacities of the HEA@CNT/$Li_{22}Sn_5$@EVA layer upon the exposure in ambient air (~30% RH) for various durations.

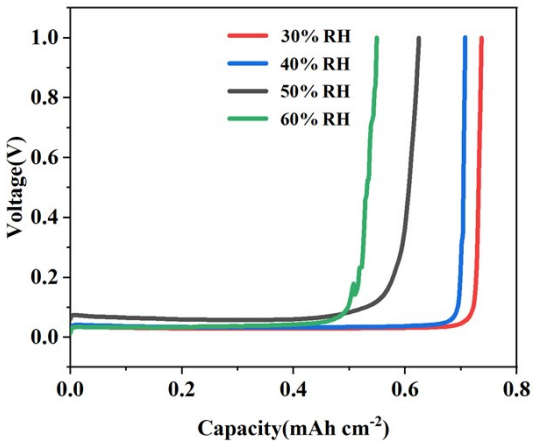

Fig. S8 Retrievable capacities of HEA@CNT/$Li_{22}Sn_5$@EVA layer for 6 h's air exposure at different relative humidity (RH) levels.

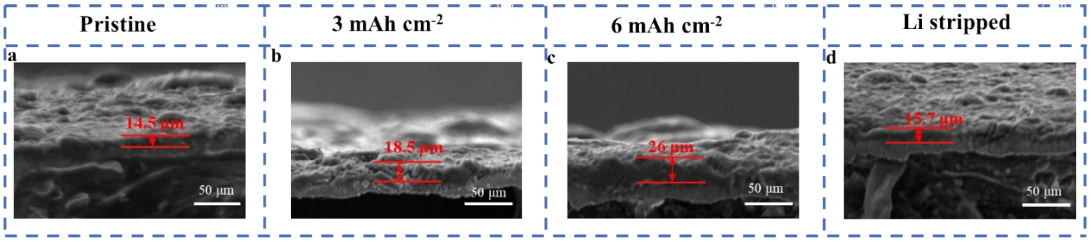

Fig. S9. (a) cross-sectional image of the pristine HEA@CNT/$Li_{22}Sn_5$@EVA electrode before the Li plating process. (b) cross-sectional image of the HEA@CNT/$Li_{22}Sn_5$@EVA electrode after the Li plating process with 3 mAh cm^{-2}. (c) cross-sectional image of the HEA@CNT/$Li_{22}Sn_5$@EVA electrode after the Li plating process with 6 mAh cm^{-2}. (d) cross-sectional image images of the HEA@CNT/$Li_{22}Sn_5$@EVA electrode after the Li stripping process.

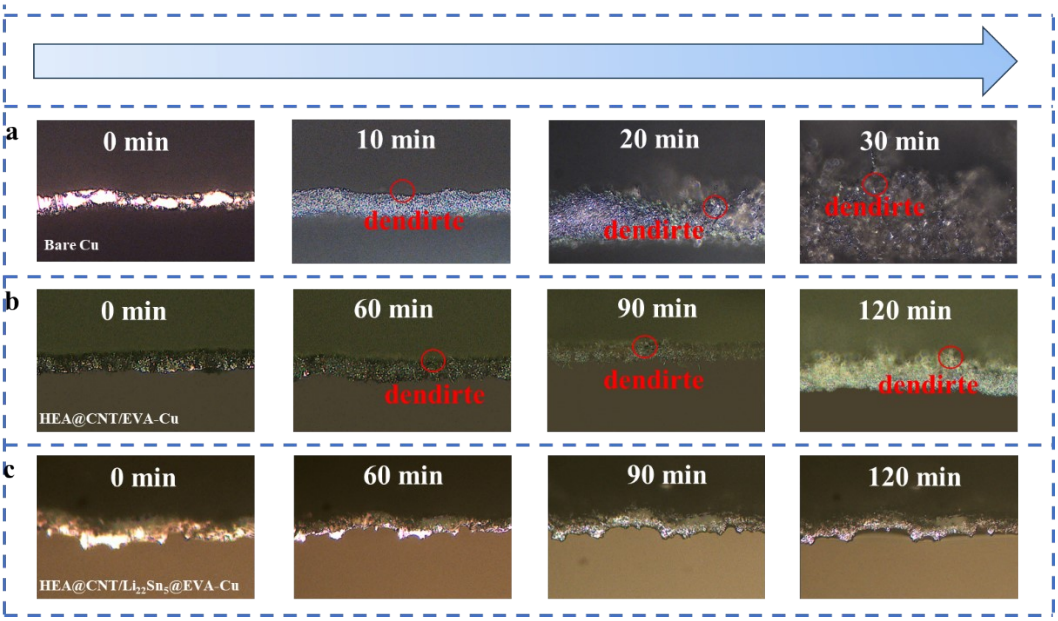

Fig. S10. In-situ optical microscopic observations of Li deposition on the (a) Cu, (b) HEA@CNT/EVA-Cu and (c) HEA@CNT/$Li_{22}Sn_5$@EVA-Cu electrodes.

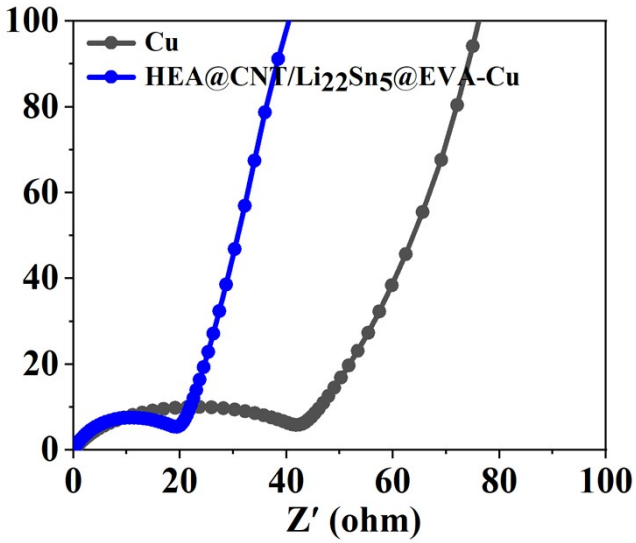

Fig. S11. Electrochemical impedance spectroscopy (EIS) of Cu and HEA@CNT/$Li_{22}Sn_5$@EVA-Cu in symmetric cells after 50 cycles.

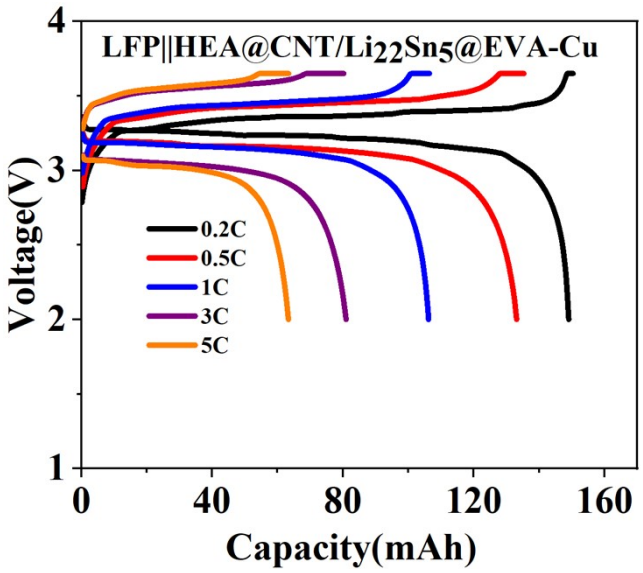

Fig. S12. Charge/discharge curves of LFP||HEA@CNT/$Li_{22}Sn_5$@EVA-Cu at different cycling rates.

When pairing HEA@CNT/$Li_{22}Sn_5$@EVA-Cu anode at the areal loading mass of 0.31 mg cm^{-2} (double side deposition) with the LFP cathode at loading mass of 25.53 mg cm^{-2} (double side deposition), the pilot-line produced pouch full-cell prototype (145 mAh) was constructed with the capacity controlled as 145 mAh, the pouch full-cell prototype was constructed. The energy density was calculated based on total mass of the whole pouch cell including active material of cathode and anode, conductive additive, current collector, separator, electrolyte and aluminum-plastic pouch by below equations by below equations:

$$\text{Gravimetric energy density (W h kg}^{-1}\text{)} = \text{specific capacity}\left(\text{mA h g}^{-1}\right) \times \text{average voltage (V)} = \frac{\text{capacity of the full cell}}{\text{weight of (cathode + anode + collector + separa}} \times \text{average voltage (V)} \quad (1)$$

$$\text{Gravimetric specific power density}\left(\text{W kg}^{-1}\right) = \text{gravimetric energy density}\left(\text{W h kg}^{-1}\right) \times \text{C rate}\left(\text{h}^{-1}\right) \quad (2)$$

The calculations are described as below:

When the C-rate is 0.2:

$$\text{Gravimetric specific capacity} = \frac{147.5\ \text{mA h}}{1.61\ \text{g}} = 91.6\ \text{mAh g}^{-1}.$$

Gravimetric energy density = (91.6 mAh g^{-1}) × (3.55 V) = 325.2 W h kg^{-1}.

Gravimetric specific power density = (325.2 W h kg^{-1}) × (0.2 h^{-1}) = 65.4 W kg^{-1}.

Table S1. The calculation results of the gravimetric energy densities and power density of the LFP||HEA@CNT/$Li_{22}Sn_5$@EVA-Cu pouch cell with ether-based localized high-concentration electrolyte (LiFSI-1.2DME-3TTE) at different C-rates (based on the total mass of the whole pouch cell).

C-rate	Energy Density (Wh Kg^{-1})	Power Density (W Kg^{-1})
0.2 C	325.2	65.4
0.5 C	282.9	141.5
1 C	242.8	242.8
3 C	163.4	490.2
5 C	120.7	603.5

Table S2. A general performance comparison of the LFP||HEA@CNT/$Li_{22}Sn_5$@EVA-Cu with ether-based localized high-concentration electrolyte (LiFSI-1.2DME-3TTE) versus state-of-the-art full devices from literatures.

Anode	Cathode	Max. Gravimetric energy density
HEA@CNT/$Li_{22}Sn_5$@EVA-Cu (this work)	LFP	325.2@0.2C
LTO[1]	LFP	110@1C
Li[2]	NCM811	300@0.1C
Ge-SWCNT-Ti[3]	LFP	210@0.1C
PLCN[4]	LFP	323.3@0.1C
Li[5]	NCM811@BNQS	321.1@0.1C
C@LTSO/CNT[6]	LFP	200@0.1C

References for Supporting Information

1. Z. Yao, X. Xia, C. a. Zhou, Y. Zhong, Y. Wang, S. Deng, W. Wang, X. Wang and J. Tu, Advanced Science, 2018, **5**, 1700786.
2. Q. Zhao, N. W. Utomo, A. L. Kocen, S. Jin, Y. Deng, V. X. Zhu, S. Moganty, G. W. Coates and L. A. Archer, *Angewandte Chemie International Edition*, 2022, **61**, e202116214.
3. A. C. R. Dileo, M. Ganter, R. Rogers, C. Cress, *ACS Nano*, 2010, **4**, 6121-6131.
4. K. Zhou, M. Zhang, X. Zhang, T. Wang, H. Wang, Z. Wang, X. Tang, M. Bai, S. Li, Z. Wang and Y. Ma, *Chemical Engineering Journal*, 2023, **464**, 142537.
5. J.-H. Kim, J.-M. Kim, S.-K. Cho, N.-Y. Kim and S.-Y. Lee, *Nature Communications*, 2022, **13**, 2514.
6. Z. Yao, X. Xia, C. a. Zhou, Y. Zhong, Y. Wang, S. Deng, W. Wang, X. Wang and J. Tu, Advanced Science, 2018, **5**, 1700786.